Fracture behaviour of diffusion bonded titanium alloys with strength mismatch

Article *in* Science and Technology of Welding & Joining · August 2002

DOI: 10.1179/136217102225004220

CITATIONS
14

READS
111

3 authors:

M. Koçak
Gedik Holding, Gedik University
186 PUBLICATIONS **2,965** CITATIONS
SEE PROFILE

Murat Pakdil
Bolu Abant Izzet Baysal University
32 PUBLICATIONS **396** CITATIONS
SEE PROFILE

Gürel Çam
Iskenderun Technical University
19 PUBLICATIONS **188** CITATIONS
SEE PROFILE

Fracture behaviour of diffusion bonded titanium alloys with strength mismatch

M. Koçak, M. Pakdil, and G. Çam

The present study considers the effect of strength mismatch on the fracture behaviour of diffusion bonded joints between commercially pure (CP) Ti and Ti–6Al–4V (Ti64), including dissimilar joints and sandwich structures with strength undermatching and overmatching. The aim of the investigation is to determine the influence of the interlayer thickness (for both higher and lower strength interlayers) and the bond quality on the deformation behaviour and fracture toughness of the joints. The influence of mechanical heterogeneity (strength mismatch) on the fracture behaviour of the interface in dissimilar joints was also investigated. Round bars of CP Ti and Ti64 having a diameter of 40 mm were diffusion bonded as dissimilar butt joints and sandwich structures containing lower strength (undermatching) and higher strength (overmatching) interlayers of different thicknesses. Round transverse tensile specimens and standard four point bend (single edge notch bend) specimens were extracted from the joints via spark erosion cutting. The four point bend specimens were fatigue precracked to introduce a sharp crack after introducing machine notches at the centre of the interlayers in the sandwich structures and at the interface in the dissimilar joints, and tested at room temperature. Some specimens were also prepared with the crack positioned away from the interface to determine the effect of notch position on fracture behaviour. The effect of strength mismatch on the crack tip opening displacement fracture toughness parameter of the joints has been evaluated. Crack initiation, crack growth, and crack deviation processes have been examined and fracture resistance curves (R curves) constructed for the joints. These results were used to explain the influence of mechanical heterogeneity of the joints and interlayer thickness on fracture behaviour. *STWJ/289*

Dr Koçak is in the GKSS Research Centre, Institute of Materials Research, Max-Planck-Straβe, D–21502 Geesthacht, Germany (mustafa.kocak@gkss.de). Mr Pakdil and Professor Çam are in the Mustafa Kemal University, Faculty of Engineering and Architecture, Mechanical Engineering Department, Tayfur Sökmen Campus, TR–31034 Antakya/Hatay, Turkey. *Manuscript received 27 September 2001; accepted 11 December 2001.*

INTRODUCTION

Many structural components produced via welding or solid state bonding contain a bimetallic interface between zones of differing mechanical behaviour. The interface can be the heat affected zone (HAZ) in fusion welded joints or the reaction zone in diffusion bonded dissimilar joints. The fracture process in such joints is determined by the intrinsic toughness of the interface region as well as the strength and toughness levels of the joined materials. However, the interface region (e.g. the fusion zone in welding) may contain flaws and can be a critical location for fracture, thus limiting the structural performance of such components. In contrast with homogeneous bodies, the joint performance is determined by the interface quality resulting from the joining process variables, the mechanical properties of the two materials joined (strength difference between them), the existence of a reaction zone or fusion zone having different mechanical properties, and the width of the region in which there is a mechanical property variation. For instance, a narrow strength overmatching fusion zone is present in autogenous laser beam welded C–Mn steels[1–4] and a strength undermatching fusion zone is observed in autogenous laser or electron beam welded precipitation strengthened Al alloys.[3–6] Therefore, a complete characterisation of the fracture process at the interface requires interfacial fracture toughness data over the full range of combinations of joining process variables, interface microstructure (if applicable), interlayer thickness, and loading mode.

The fracture mechanics of elastic–plastic bimaterial interfaces (where one of the constituents may deform plastically) has recently been the focus of research[7–18] to improve the understanding of the fracture process at such bimaterial interfaces. It is now well established that deformation and fracture behaviour is significantly affected by the strength mismatch between the two materials joined.[19,20] Recently, Kim *et al.*[21,22] have conducted numerical work and slip line field analysis on bimaterial single edge bend and centre cracked tension configurations. Their results showed the development of about 38% higher triaxiality at the interface compared with homogeneous specimens.

For experimental evaluation of the interfacial fracture toughness of similar or dissimilar joints, four point bending tests are generally used since this type of loading (constant bending moment) provides a condition (a steady state energy release rate) that facilitates the acquisition of accurate and consistent fracture resistance data[10] for interface testing using flexural specimens. The bimaterial elastic–plastic specimens can be produced via the solid state diffusion bonding process. These dissimilar joints may fail either by brittle debonding of interfaces (weak bonding) or by crack deviation into the lower strength constituent and ductile rupture within the lower strength side adjacent to the interface (strong bonding).[23,24] Sandwich specimens basically contain a thin layer of interlayer (material I) which is sandwiched between the two solid blocks (material II) comprising the bulk of the specimen. This type of specimen can also be produced via the solid state diffusion bonding process. A sandwich structure comprising a lower strength metal (undermatching) interlayer between higher strength metal blocks may fail via a variety of mechanisms, including brittle debonding of interfaces and ductile rupture within the interlayer adjacent to the interface. The fracture process

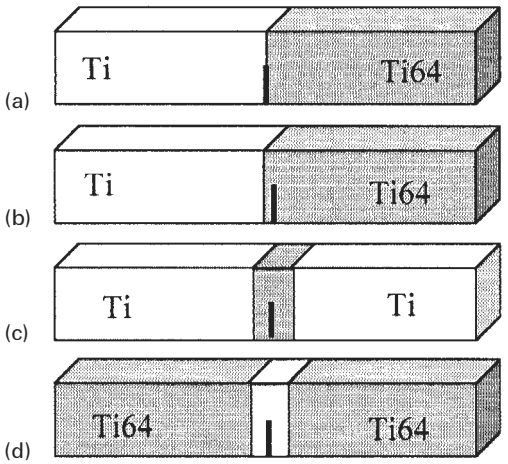

a dissimilar joint with interfacial crack; *b* dissimilar joint with subinterfacial crack; *c* strength overmatched joint; *d* strength undermatched joint

1 Schematic diagrams showing fracture toughness specimens

for such joints depends on the level of elastic/plastic mismatch, and the interlayer thickness $2H$ and uncracked ligament size $(W-a)/2H$, where W is the specimen width and a is the initial crack length. In contrast, crack deviation into the lower strength material side is expected in overmatching (higher strength interlayer) sandwich structures where the crack is located in the higher strength interlayer, provided that the interlayer is thin enough, the bond quality is high enough, and there is sufficient strength overmatching.

In the present study, a commercial purity (CP) Ti and Ti–6Al–4V (Ti64) material combination is used to conduct a systematic experimental investigation on the elastic–plastic

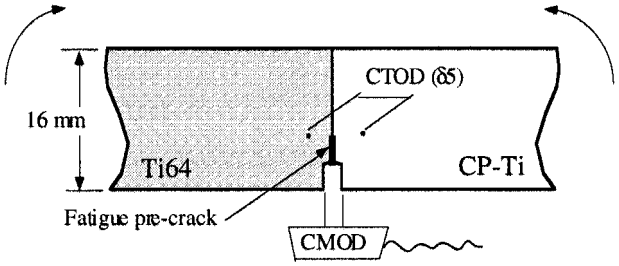

2 Schematic illustration of crack tip opening displacement (CTOD δ_5) measurement during four point bend tests using clip on gauge with 5 mm gauge length over fatigue crack tip

interface fracture. The reason for selecting this model joint system is twofold. First, these two materials can readily be diffusion bonded to each other. Second, these materials exhibit identical elastic properties with significantly different yield stress levels, resulting in a high strength mismatch ratio, i.e. about 300%. Joints between these two materials exhibiting only a strength mismatch and free from any microstructural change can readily be achieved provided that excessive grain growth and interdiffusion can be avoided at the bond interface by selecting an appropriate set of diffusion bonding parameters. Sandwich joints with strength undermatching and overmatching interlayers produced in the present study represent model joints for laser beam or conventional arc welded joints. Laser beam welded precipitation hardened Al alloys with an undermatching weld zone and structural steel or Ti alloy joints with an overmatching weld zone can be simulated by these undermatching and overmatching sandwich joints, respectively.

The aim of the present work was to carry out a comprehensive experimental programme to improve the understanding of fracture toughness behaviour under the influence of strength mismatch. For this purpose, fracture

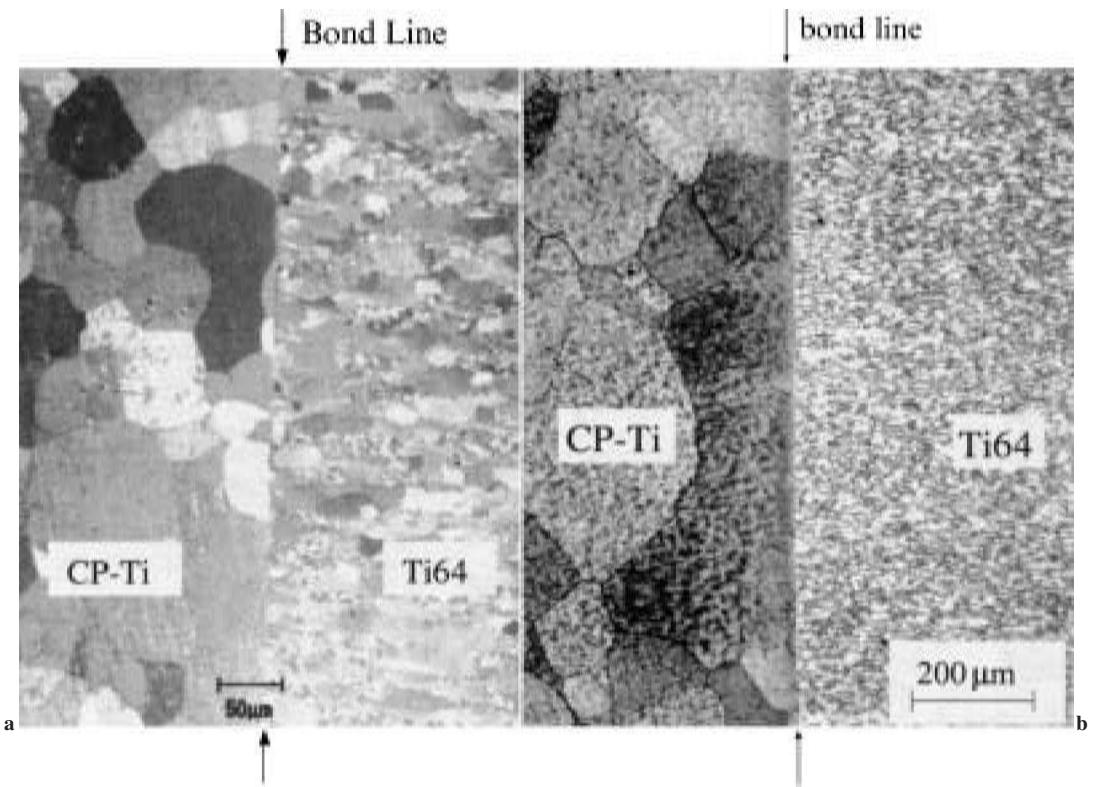

a weak bond, polarised light image; *b* strong bond, light image

3 Microstructure of bond lines (optical)

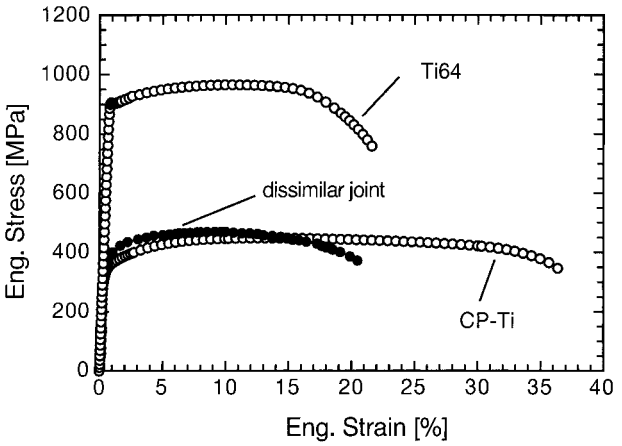

4 Stress–strain curves for base materials and dissimilar joint used in present study

toughness tests were carried out on dissimilar Ti–Ti64 diffusion bonded butt joints and sandwich specimens to determine the effect of strength mismatch on fracture behaviour and crack tip opening displacement (CTOD) R curves. In the sandwich joints, the effect of interlayer thickness on the fracture behaviour of joints with both undermatching and overmatching of strength was also investigated.

EXPERIMENTAL PROCEDURE

The fracture behaviour of diffusion bonded CP Ti and Ti64 joints formed via solid state diffusion bonding was examined. For this purpose, 40 mm diameter bars of Ti (99·5%) and Ti64 were diffusion bonded in different combinations, such as dissimilar butt joints and sandwich specimens, to produce undermatched and overmatched sandwich structures with different interlayer thicknesses. Dissimilar joints and sandwich structures were joined using bonding parameters of 875°C and 5 MPa with a bonding time of 1 h, using surfaces that had been ground and polished followed by degreasing in an ultrasonic washer and blow drying. Sandwich structures were also produced at 870°C and 3·5 MPa with a bonding time of 1 h after only parallel machining and degreasing in an ultrasonic washer followed by rinsing in pure ethanol and blow drying, to produce relatively weak interfaces. The vacuum level at bonding temperature T_b was 4×10^{-6} mbar (3×10^{-6} torr) or better. These bonding parameters were selected to obtain a well defined bond line without producing a reaction zone, to eliminate the effect of the latter.

Optical metallography and scanning electron microscopy were also used to inspect the quality of the bonds produced

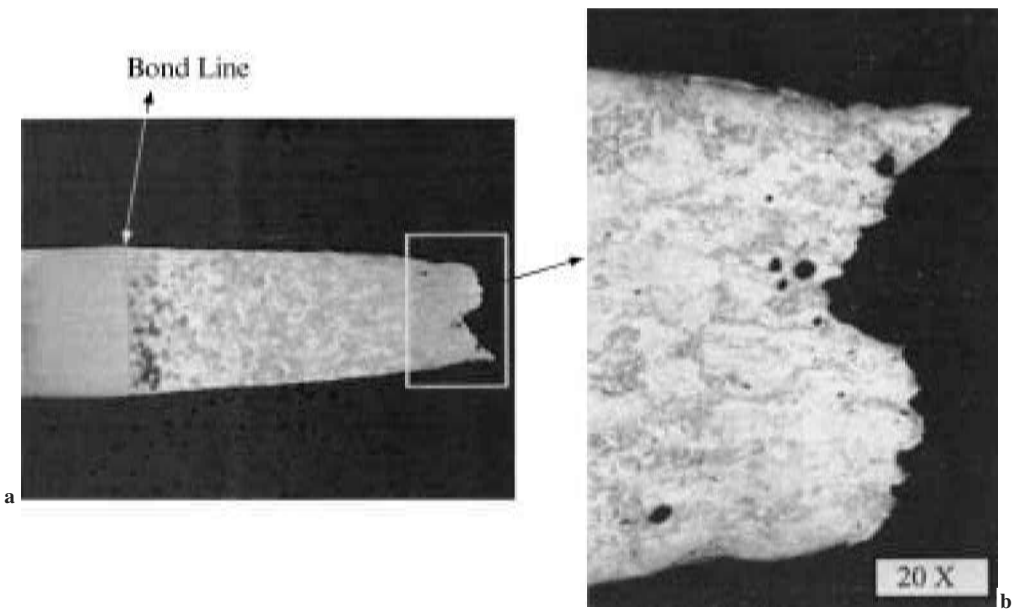

a overview; *b* higher magnification of failure location

5 Tensile specimen of diffusion bonded dissimilar joint, which failed in lower strength commercial purity (CP) Ti side away from interface (optical)

Table 1 Tensile test results for base materials and dissimilar joint

Material	Yield strength, MPa		Tensile strength, MPa		Strain, %	
	Experimental	Average	Experimental	Average	Experimental	Average
CP Ti	320	332	431	445	30·0	35·2
	342		456		39·6	
	335		448		36·0	
Ti64	903	923	965	977	22·0	21·7
	937		986		22·0	
	930		981		21·0	
Dissimilar joint*, $M=0{\cdot}36$	339	340	438	458	19·4	19·3
	346		458		18·4	
	336		479		20·3	

*Transverse tensile specimen: mismatch ratio $M = YS_{CP\ Ti}/YS_{Ti64}$, where YS is yield strength.

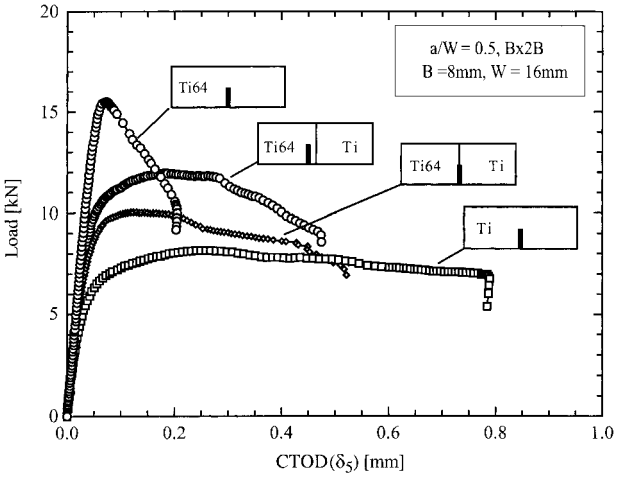

6 Load versus CTOD δ_5 plots for base materials and dissimilar joints

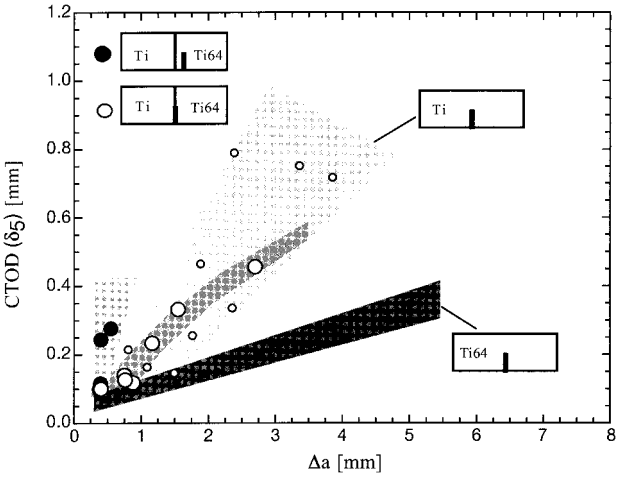

7 Comparison between *R* curves (CTOD δ_5 versus increase in crack length Δa) for base materials and dissimilar joints

and to characterise the diffusion bonded interface between CP Ti and Ti64.

Standard round tensile specimens were extracted from the base metals and dissimilar joints using the spark erosion technique and tested at room temperature. Fracture toughness test specimens of 8 or 10 mm thickness with $B \times 2B$ specimen geometry (Fig. 1) were also extracted from the bonded joints. The specimens were machine notched (using spark erosion with 0·2 mm diameter Cu wire) at the interface (some specimens with notches in Ti64 away from the interface, i.e. subinterfacial crack specimens, were also produced) and fatigue precracked to contain deep notches ($a/W = 0{\cdot}5$). Fracture toughness tests using these fatigue precracked four point bending specimens of CP Ti and Ti64 bulk materials were also conducted to determine their bulk toughness values. As usual, load and crack mouth opening displacement (CMOD) values were recorded during the testing. Additionally, CTOD values were directly measured using δ_5 (developed at GKSS) clip on gauges at the fatigue crack tip over a gauge length of 5 mm (Fig. 2). This local CTOD measurement technique may monitor the crack tip deformation and fracture process in dissimilar joints more precisely than the remote displacement measurement. However, the 5 mm gauge length used is greater than the interlayer thickness of some of the sandwich specimens (*see* Table 3).

Table 2 Crack tip opening displacement (CTOD δ_5) values at maximum load for base materials and dissimilar joints

Material	CTOD δ_{5max}, mm	
	Experimental	Average
Bulk CP Ti	0·21	0·22
	0·24	
	0·21	
Bulk Ti64	0·07	0·06
	0·06	
	0·06	
	0·07	
	0·06	
	0·06	
Dissimilar joint (interfacial crack), crack geometry I (Fig. 1*a*)	0·09	0·10
	0·12	
	0·10	
	0·11	
	0·11	
	0·08	
	0·10	
	0·14	
	0·08	
	0·08	
	0·10	
	0·12	
Dissimilar joint* (subinterfacial crack), crack geometry II (Fig. 1*b*)	0·17	0·18
	0·18	
	0·20	

*Specimen showed crack deviation from crack tip into Ti64 side (*see* Fig. 8*b*).

RESULTS AND DISCUSSION

Microstructural aspects and tensile behaviour of dissimilar joints

A distinct and well defined bond line between CP Ti and Ti64 was produced in all the joints. Neither bond defects nor grain growth were observed in both materials in the bond zone, as shown in Fig. 3. In the sandwich structures with relatively weak interfaces, optical microscopy did not reveal any detectable bonding defects. Indeed, the interface of these bonds seemed very similar to that obtained in the strong bond joints (Fig. 3*a* and *b*).

Tensile tests on the CP Ti and Ti64 bars used in the present work were carried out to determine the tensile properties and the strength mismatch ratio. The mismatch factor $M = \text{YSCP Ti}/\text{YS}_{\text{Ti64}}$, where YS is yield strength, was found to be 0·36. An average of four tests was taken to determine the yield strengths and ultimate tensile strengths of CP Ti and Ti64. The stress–strain curves for these materials are compared in Fig. 4.

The stress–strain curve for the dissimilar joint with a strong bond was also determined and is compared with those for the constituent base materials in Fig. 4. As can be seen from Fig. 4 and Table 1, the strength value for the joint is similar to that for CP Ti base material, but the failure strain value for the joint is almost half that for CP Ti base material, as is expected since only the lower strength CP Ti side (half of the gauge length) deforms plastically during tensile testing. The tensile specimens from the dissimilar joints all failed in the lower strength CP Ti side away from the bond interface as shown in Fig. 5, indicating that the bond is sound. The bonds failing in the softer CP Ti side away from the bond line in tensile testing will subsequently be termed 'strong bonds', whereas those failing along the bond line will be designated as 'weak bonds'.

Fracture behaviour

A multiple specimen technique using four point bend specimens was employed to determine the CTOD *R* curves

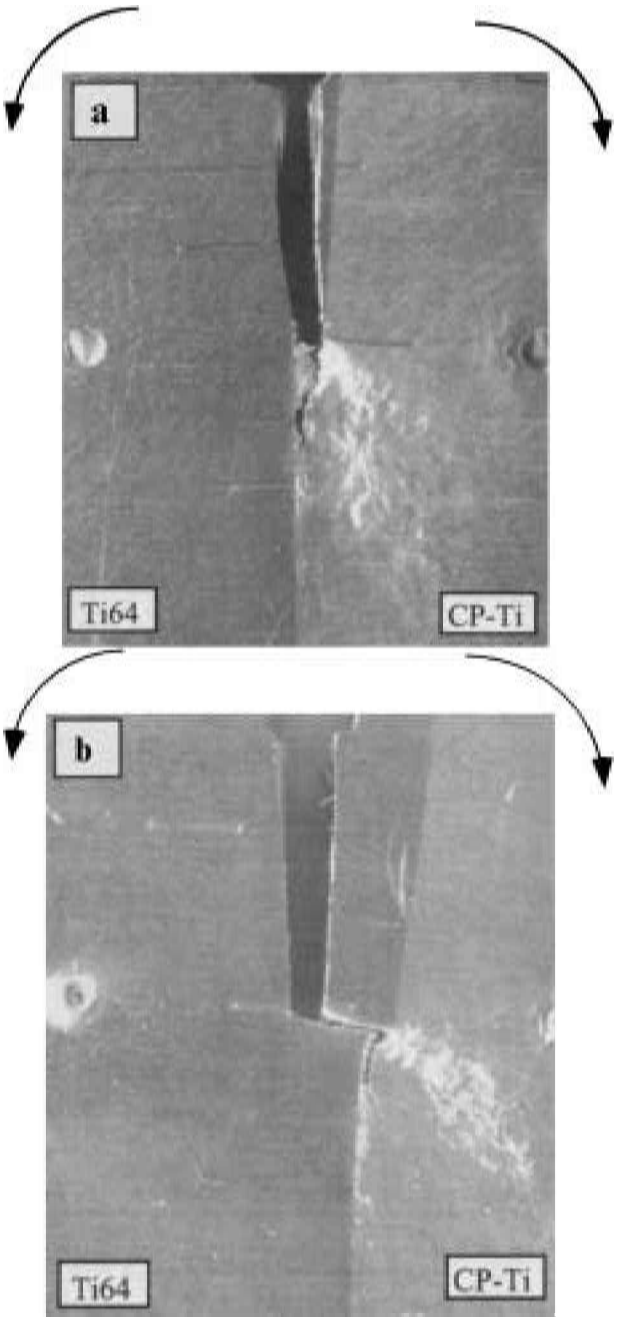

a interfacial crack specimen, in which ductile crack growth occurs within CP Ti adjacent to interface; *b* subinterfacial crack specimen, in which crack grows perpendicular to interface and deviates into lower strength CP Ti, with subsequent ductile fracture within CP Ti adjacent to interface

8 Crack growth in strong bond dissimilar joint specimens (optical)

for the base materials and dissimilar joints. The measured CTOD values (δ_{5max} corresponding to the CTOD values at maximum load) for the base materials and dissimilar joints are given in Table 2. As can be seen from this table, the CTOD values for the dissimilar joints lie between those for homogeneous CP Ti and Ti64. Figure 6 shows the typical load versus CTOD (δ_5) plots obtained for bulk materials and diffusion bonded interface and subinterface crack specimens. The variations in load carrying capacity demonstrate the effect of the material strength and the notch position.

Figure 7 shows the *R* curves for the base materials and dissimilar joint specimens. The *R* curve behaviour for dissimilar joints with interfacial cracks is similar to that for

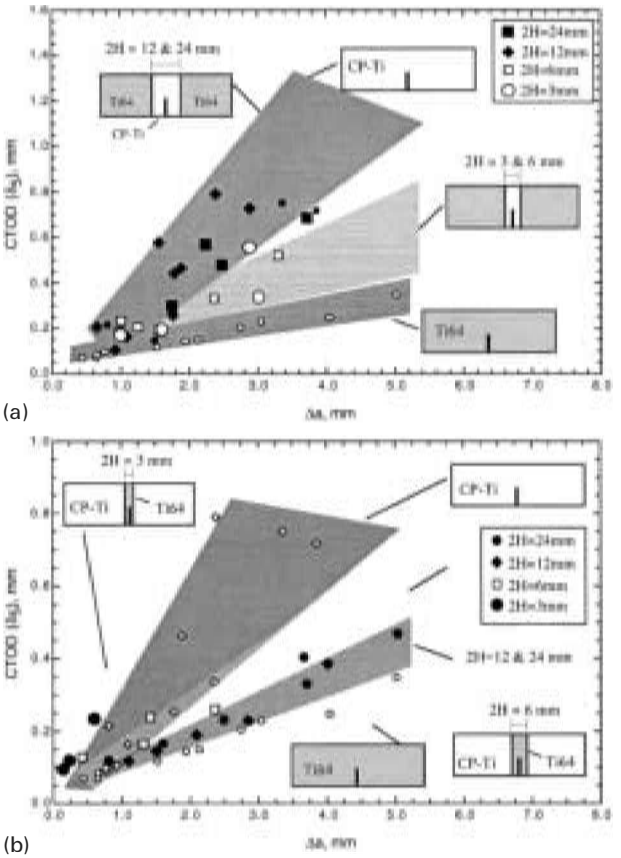

9 Effect of interlayer thickness on *R* curves for *a* undermatched and *b* overmatched specimens with weak bond

homogeneous CP Ti. In these specimens, the crack moves from the interface into the lower strength CP Ti side and propagates adjacent to the interface (Fig. 8*a*) owing to the incompatibility between the plastic properties of the two materials. In contrast, the *R* curve for dissimilar joints with subinterfacial cracks lies higher than that for CP Ti. The reason for this ambiguity is that the original fatigue precrack lying in Ti64 deviates into the lower strength CP Ti side (via perpendicular crack growth to the interface) under bending owing to the presence of an extreme strength overmatch (Fig. 8*b*) and this extensive crack deviation leads to an artificial increase in the CTOD value. Table 2 also gives the rather high CTOD results for the subinterfacial crack specimens (*see* Fig. 1*b*). This is partly due to the crack growth (perpendicular to the interface, i.e. non-mode I crack tip opening) parallel to the local CTOD measurement direction as shown in Fig. 8*b*. Furthermore, a greater amount of deformation occurs in the specimen to link the subinterfacial crack tip (within the higher strength Ti64) to the plastically deformed interfacial region (Fig. 8*b*). The crack path deviation towards the interface in subinterfacial crack specimens was also observed in an earlier work[14] conducted on an explosion clad Cu–ferrite system.

The measured CTOD values (δ_{5max}) for the base materials and undermatched and overmatched bonded joints are compared in Table 3. It can be seen from this table that in the undermatching system a decreasing interlayer thickness decreases the CTOD with respect to that for homogeneous CP Ti. The reason for this is the restrictions in plasticity development (increase of constraint) at the uncracked ligament due to the presence of higher strength Ti64 blocks on both sides. The thin, lower strength CP Ti interlayer is restrained by the non-deforming Ti64 side blocks, which has the effect that the effective yield strength of CP Ti is significantly increased (contact strengthening); this is also

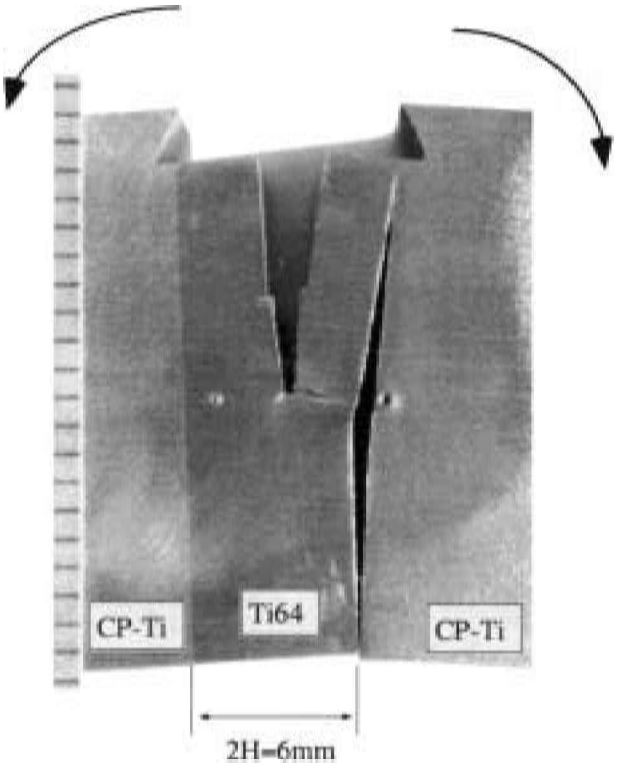

10 Crack deviation from stronger Ti64 interlayer into softer CP Ti side block and brittle debonding along interface due to weak bonding in strength overmatched weak bond specimen with interlayer thickness $2H=6$ mm (optical)

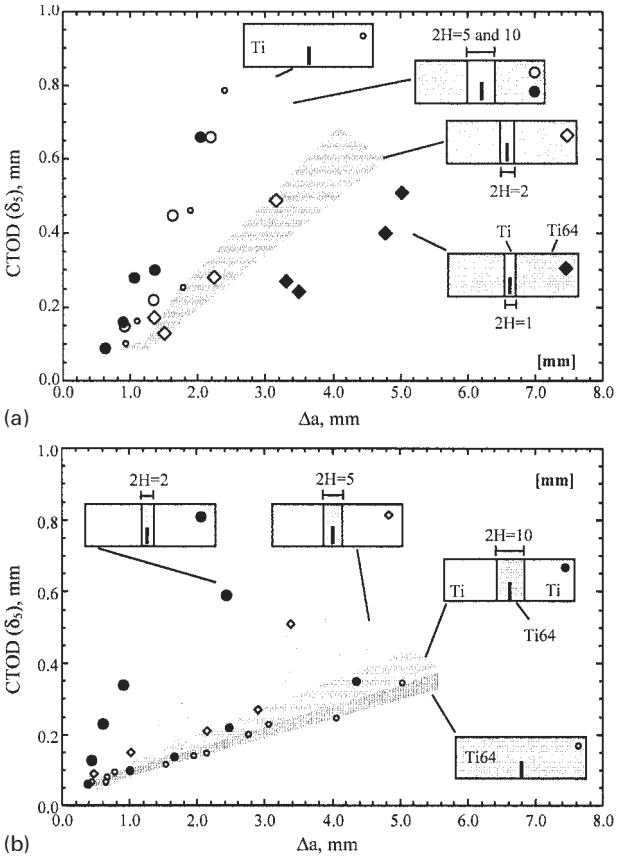

11 Effect of interlayer thickness on *R* curves for *a* undermatched *b* overmatched specimens with strong bond

observed in brazed joints.[25] The constrained plasticity has also been observed in Ti–Al–Ti diffusion bonds with a soft Al interlayer in a previous work.[26] The opposite tendency was observed for the overmatching system as expected, where decreasing interlayer thickness increases the CTOD as the contribution from the lower strength CP Ti side blocks becomes more pronounced.

The multiple specimen technique using four point bend tests was employed to determine the *R* curves for the base materials and undermatched and overmatched sandwich joints having both weak and strong bonds. Figure 9*a* and *b* shows the effect of interlayer thickness on the *R* curve behaviour for specimens having weak bonds and undermatched and overmatched interlayers respectively, in comparison with those for the base materials. The *R* curve behaviour for undermatched specimens becomes similar to that for homogeneous Ti64 as the interlayer thickness decreases to 3 mm (within experimental scatter bands). In contrast, the *R* curve behaviour for overmatched specimens becomes

Table 3 Comparison of CTOD δ_{5max} values for homogeneous CP Ti and Ti64, and undermatched and overmatched specimens with weak and strong bonds

Bonded specimens	Interlayer thickness $2H$, mm	Uncracked ligament size/interlayer thickness $(W-a)/2H$	CTOD δ_{5max} values*, mm	Bulk base material CTOD, mm
Weak bonds				
Undermatched specimens	3	3·3	0·12	0·22 (CP Ti)
(CP Ti interlayer)	6	1·6	0·13	
	12	0·8	0·17	
	24	0·4	0·17	
Overmatched specimens	3	3·3	0·21	0·06 (Ti64)
(Ti64 interlayer)	6	1·6	0·10	
	12	0·8	0·09	
	24	0·4	0·10	
Strong bonds				
Undermatched specimens	1	8·0	0·07	0·22 (CP Ti)
(CP Ti interlayer)	2	4·0	0·09	
	5	1·6	0·12	
	10	1·0	0·17	
Overmatched specimens	2	4·0	0·15	0·06 (Ti64)
(Ti64 interlayer)	5	1·6	0·08	
	10	1·0	0·07	

*Average of minimum 3 specimens.

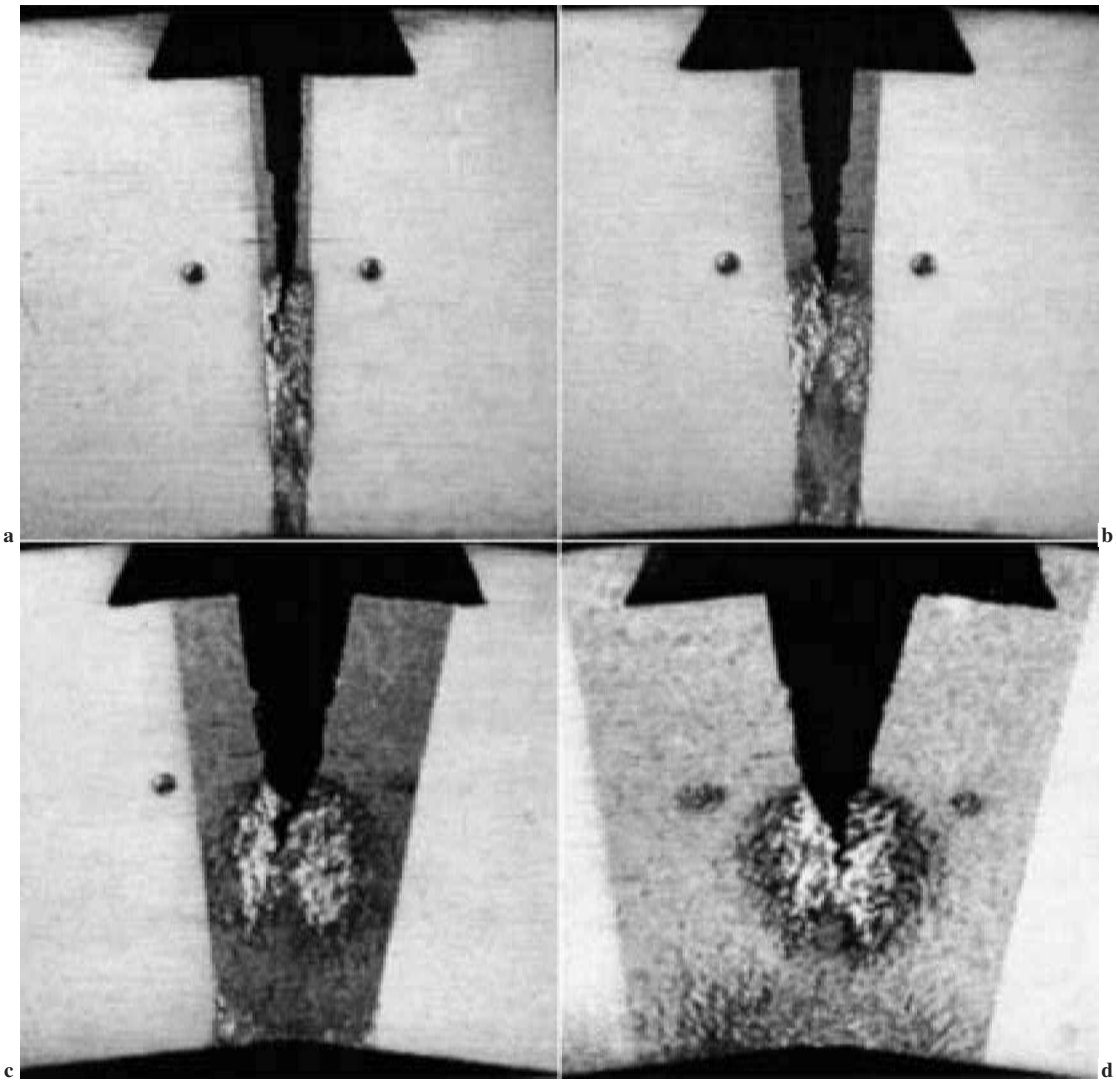

12 Crack growth in strength undermatched strong bond specimens with interlayers of thickness *a* $2H=1$ mm, *b* $2H=2$ mm, *c* $2H=5$ mm, and *d* $2H=10$ mm (optical)

similar to that for CP Ti as interlayer thickness decreases owing to remote plasticity development in the lower strength CP Ti material. In the undermatched sandwich structures, the specimens failed in the softer CP Ti interlayer away from the interface except for one specimen having a 3 mm interlayer thickness, despite the weakness of the interface. This is probably due to the supporting effect of the non-deforming Ti64 side blocks (contact strengthening). However, as can be seen from Fig. 9*b*, only very limited CTOD data were obtained for weak bond overmatched sandwich joints with interlayer thicknesses of 3 and 6 mm. The reason for this is the brittle debonding along the weak interfaces that occurs in these specimens as the crack lying in the higher strength Ti64 interlayer deviates into the lower strength side block via the weak interface, as shown in Fig. 10.

Similar observations were made on the R curve behaviour for undermatched and overmatched sandwich joints with strong bonds (Fig. 11). It was, however, possible to obtain more CTOD data for strong bond overmatched sandwich joints with small interlayer thicknesses (i.e. 2 and 5 mm). For the strong bond specimens, brittle debonding along the interface does not occur since the crack deviates into the lower strength side block via the strong bond and propagates in the lower strength material adjacent to the interface.

It should be mentioned that the CTOD values presented in this section were obtained directly from local measurements across the crack tip using a clip on gauge with a 5 mm gauge length, which is greater than the thickness of the thin interlayer used in the experiments. However, an identical relationship between the two displacement measurements, namely, CMOD and CTOD (δ_5), for all dissimilar and sandwich specimens with different interlayer thicknesses has been observed and hence the possible effect on the presented R curves of materials covered within the gauge length of the δ_5 clip on gauge should be not significant. Figures 7 and 9 do indeed show the expected variation, with some scatter due more to the fracture path deviation than to the material heterogeneity within the gauge length monitored across the crack tip.

Fracture process

Optical metallography was employed to investigate the fracture process in the tested specimens by sectioning them in the middle. Plastic deformation predominantly occurs in the lower strength interlayer adjacent to the interfaces for the undermatched specimens, as shown in Fig. 12. The shape of plastic zone developed is determined by the thickness of the lower strength interlayer for strength undermatching (Fig. 12). A typical butterfly shaped plastic zone is formed in the specimens having sufficiently thick interlayers (Fig. 12*c* and *d*), whereas in the specimens having thin interlayers the plastic zone is confined to the lower strength

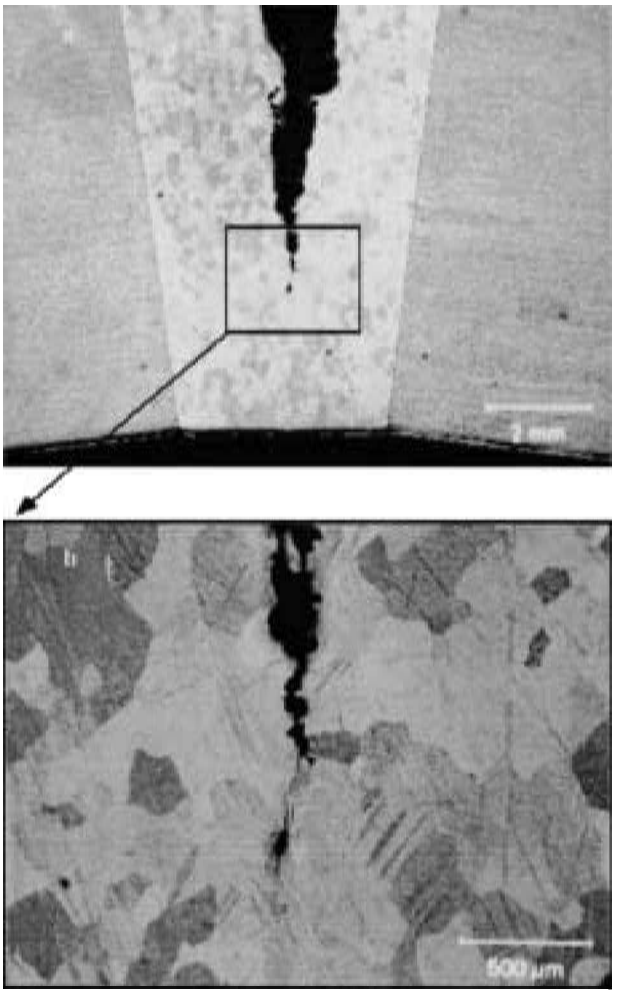

13 Crack growth involving void formation and coalescence in softer interlayer of strength undermatched strong bond specimen with interlayer thickness of 5 mm (optical)

interlayer (constrained plasticity) owing to the restrictions in plasticity development caused by the presence of higher strength (elastic) Ti64 blocks on both sides. The mode of failure was observed to be typically ductile, involving void nucleation and coalescence (Fig. 13). For overmatched specimens, the crack path deviation into the lower strength CP Ti side block and ductile failure in the lower strength side block adjacent to the interface were observed provided that the higher strength interlayer was sufficiently thin, i.e. 5–6 mm, and the bond is sound (Fig. 14*a* and *b*). No crack deviation into the lower strength side block was observed for overmatched specimens having a thicker interlayer, i.e. 10 mm, since the outer bound of the plastic zone developed cannot reach the interface (Fig. 14*c*). After the crack deviation into the lower strength CP Ti side in strength overmatched specimens having thinner interlayers, the failure occurs in a ductile manner, involving void nucleation and coalescence as observed in the strength undermatched specimens (Fig. 15).

Two types of bond quality (weak and strong depending on the failure location in tensile tests) have been covered within the present study to examine experimentally the failure mechanism at the boundaries of the interlayer material in the sandwich specimens. A higher strength interlayer represents strength overmatching weld metal, where plastic zone development concentrates at the base metal side of the interface. An accumulation of this plasticity increases the constraint in the vicinity of the interface and may lead to

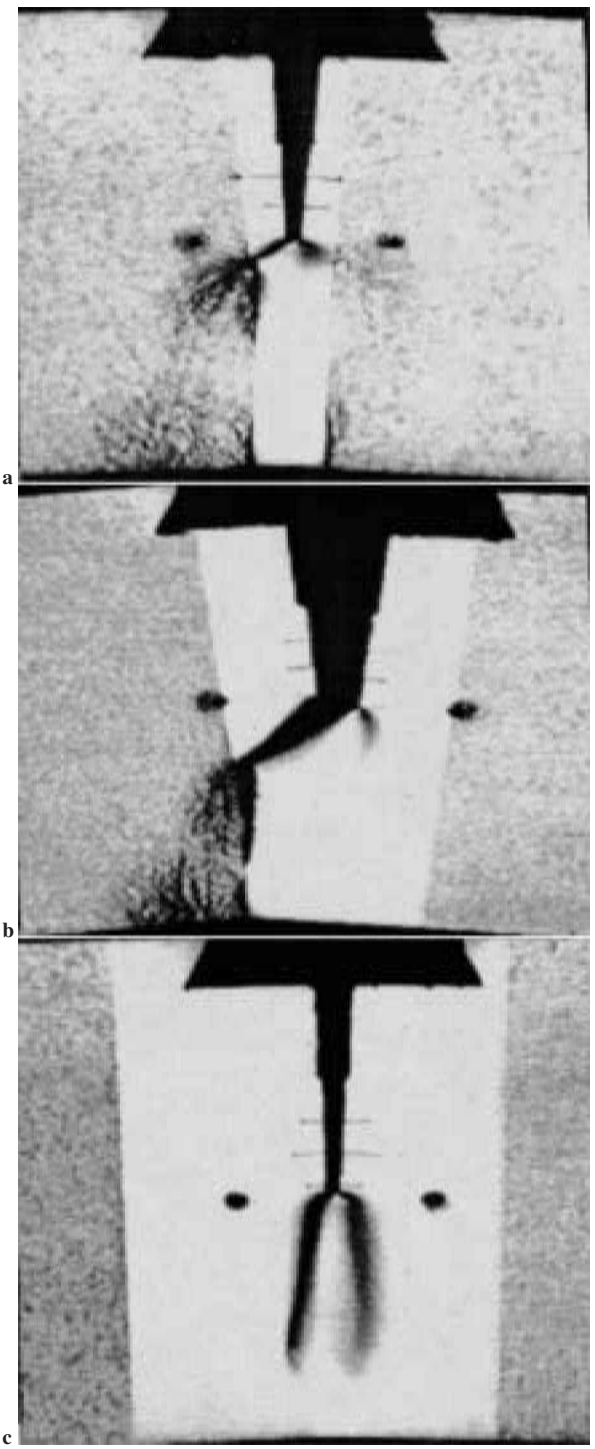

14 Crack growth in strength overmatched strong bond specimens with interlayers of thickness *a* $2H=2$ mm, *b* $2H=5$ mm, and *c* $2H=10$ mm (optical)

brittle fracture initiation if the appropriate microstructure at the interface is present. By introducing weak and strong bond qualities to the experimental matrix, it was intended to examine the critical condition for the interface with undermatching and overmatching interlayer materials under bending loading.

For the weak bonds, however, the overmatched specimens failed at the interface by brittle debonding after a certain amount of bending as the crack reached the weak interface (Fig. 10), owing to the brittle nature of the weak bonding. In contrast, no debonding was observed in undermatched specimens despite the presence of a weak bond.

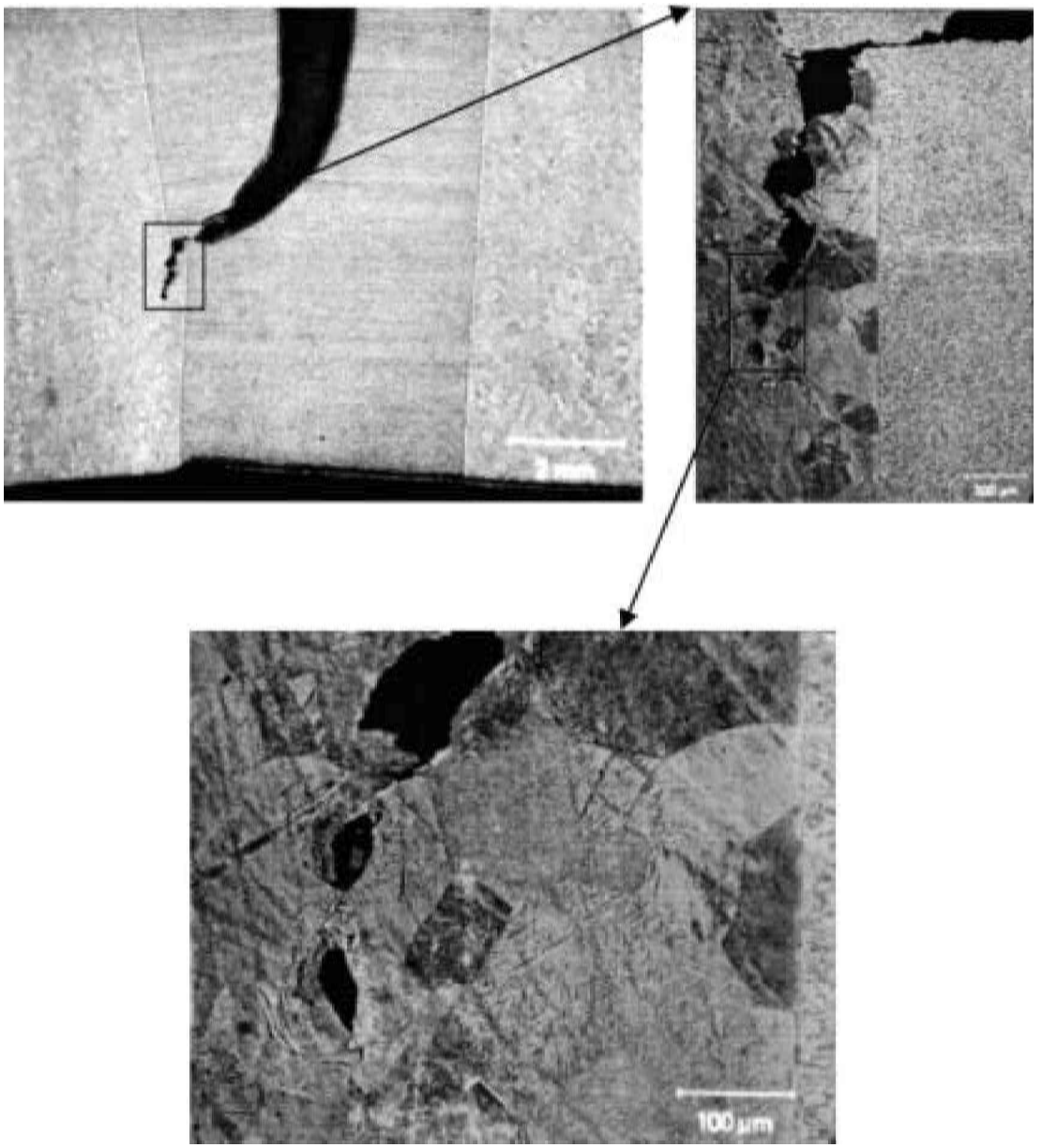

15 Crack path deviation into lower strength side block (CP Ti) and crack growth involving void formation and coalescence within side block adjacent to interface in strength overmatched strong bond specimen with interlayer thickness of 5 mm (optical)

This indicates that the form of plasticity development within the lower strength interlayer does not create a critical condition for the bond line and hence the weak bond interface does not fail. Figure 16 shows the schematic diagrams of the different fracture types (crack propagation) observed in the present study.

CONCLUSIONS

Dissimilar butt joints with strong bonds

1. Transverse tensile specimens of dissimilar joints all failed in a ductile manner in the lower strength CP Ti side, indicating that the bond quality was optimal.

2. The CTOD (δ_{5max}) values for dissimilar joint specimens lay in between those for CP Ti and Ti64 base metals.

3. The R curve for dissimilar joint specimens with an interfacial crack was found to be similar to that for CP Ti, whereas that for specimens with a subinterfacial crack lay higher, owing to the perpendicular crack growth towards the interface under bending conditions resulting from the presence of an extreme strength overmatch, thus leading to an artificial increase in the CTOD value.

4. Ductile crack growth occurred within the lower strength CP Ti side adjacent to the interface in the dissimilar joint specimens with an interfacial crack, whereas an excessive crack path deviation into the lower strength CP Ti side was observed in dissimilar joint specimens with a subinterfacial crack, with subsequent ductile crack growth within the lower strength CP Ti side adjacent to the interface.

Sandwich joints

1. The undermatched specimens all failed in a ductile manner in the softer CP Ti interlayer adjacent to the interface, not by brittle debonding along the interface, for both weak and strong bond conditions except for one weak bond specimen.

2. In the strong bond overmatched specimens with thinner interlayers, the crack originally lying in the higher strength interlayer deviated into the lower strength side

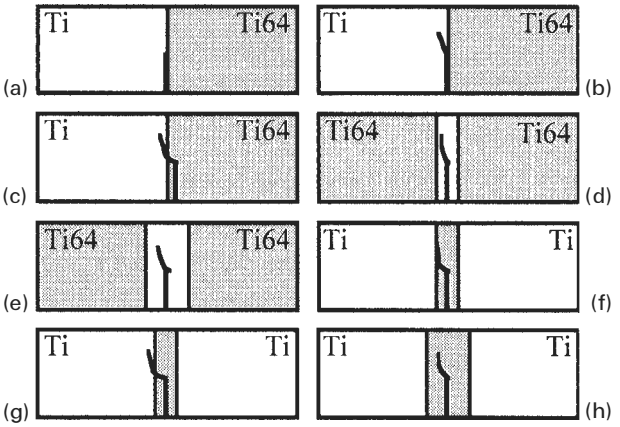

a dissimilar interfacial crack specimen with weak bond, brittle debonding along interface; *b* dissimilar interfacial crack specimen with strong bond, crack path deviation into softer CP Ti side; *c* dissimilar subinterfacial crack specimen with strong bond, crack path deviation into softer CP Ti side; *d* strength undermatched specimens with weak and strong bonds with thinner interlayers, crack propagation within softer CP Ti interlayer adjacent to interface; *e* strength undermatched specimens with weak and strong bonds with thicker interlayers, crack propagation within softer CP Ti interlayer away from interface; *f* strength overmatched specimens with weak bond with thinner interlayers, perpendicular crack growth towards interface with subsequent brittle debonding along interface; *g* strength overmatched specimens with strong bond with thinner interlayers, crack path deviation into softer CP Ti side block; *h* strength overmatched specimens with weak and strong bonds with thicker interlayers, crack propagation within stronger Ti64 interlayer away from interface

16 Crack growth mechanisms in dissimilar and sandwich joints investigated

block and propagated within the lower strength side adjacent to the interface.

3. For the weak bonding, however, overmatched specimens with thinner interlayers, e.g. 3 and 6 mm, failed at the interface after a certain amount of bending owing to the weakness of the interface, without crack tip penetration into the lower strength CP Ti material.

4. In the undermatched specimens, decreasing lower strength interlayer thickness shifted the R curve lower, towards that for Ti64, owing to the constrained plasticity.

5. In the overmatched specimens, decreasing interlayer thickness produces a shift in the R curves to higher values as a result of the increasing remote plasticity at the lower strength CP Ti side blocks.

6. The ductile crack growth was confined to the lower strength interlayer adjacent to the interface in the undermatched specimens, whereas deviation of the crack path into the lower strength CP Ti side blocks was observed in the overmatched specimens with thinner Ti64 interlayers, the final failure being either brittle debonding along the bond line for the weak bonding or ductile crack growth within the softer CP Ti side block adjacent to the bond line for the sound bonding.

ACKNOWLEDGEMENTS

The authors would like to thank Mr K.-H. Bohm, Mr S. Riekehr, and Mr H. Mackel for their technical assistance and Mrs P.-M. Fischer and Mrs W.-V. Schmitz for their help with optical microscopy. Part of this work was carried out within the German–Turkish joint project financed by International Bureau, KFA, Jülich, Germany and Tubitak, Ankara, Turkey. The authors also thank both organisations for their financial support.

REFERENCES

1. G. ÇAM, Ç. YENI, S. ERIM, V. VENTZKE, and M. KOÇAK: *Sci. Technol. Weld. Joining*, 1998, **3**, (4), 177–189.
2. G. ÇAM, M. KOÇAK, and J. F. DOS SANTOS: *Weld. World*, 1999, **43**, (2), 13–26.
3. J. F. DOS SANTOS, G. ÇAM, F. TORSTER, A. INSFRAN, S. RIEKEHR, V. VENZTKE, and M. KOÇAK: *Weld. World*, 2000, **44**, (6), 42.
4. G. ÇAM and M. KOÇAK: *Int. Mater. Rev.*, 1998, **43**, (1), 1–44.
5. G. ÇAM, V. VENTZKE, J. F. DOS SANTOS, M. KOÇAK, G. JENNEQUIN, and P. GONTHIER-MAURIN: *Sci. Technol. Weld. Joining*, 1999, **4**, (5), 317–323.
6. G. ÇAM, V. VENTZKE, J. F. DOS SANTOS, M. KOÇAK, G. JENNEQUIN, P. GONTHIER-MAURIN, M. PENASA, and C. RIVEZLA: *Prakt. Metallogr.*, 2000, **37**, (2), 59–89.
7. G. ÇAM, L. HEIKINHEIMO, M. SIREN, D. DOBI, and M. KOÇAK: Proc. Conf. 'LÖT '95', DVS Bericht 166, 233–238; 1995, Düsseldorf, Germany, Deutscher Verlag für Schweißtechnik (DVS).
8. G. ÇAM, L. HEIKINHEIMO, M. SIREN, D. DOBI, and M. KOÇAK: Proc. 4th Int. Conf. on 'Trends in welding research', Gatlinburg, TN, June 1995.
9. B. J. DALGLEISH, K. P. TRUMBLE, and A. G. EVANS: *Acta Metall.*, 1989, **37**, (7), 1923–1931.
10. Z. SUO and J. W. HUTCHINSON: *Mater. Sci. Eng.*, 1989, **A107**, 135–143.
11. I. E. REIMANIS, B. J. DALGLEISH, M. BRAHY, M. RÜHLE, and A. G. EVANS: *Acta Metall. Mater.*, 1990, **38**, (12), 2645–2652.
12. E. TSCHEGG, H. O. K. KIRCHNER, and M. KOÇAK: *Acta Metall. Mater.*, 1990, **38**, (3), 469–478.
13. C. F. SHIH, R. J. ASARO, and N. P. ODOWD: Proc. Scr. Metall. Conf. on 'Bonding, structural and mechanical properties', 313–325; 1990, Elmsford, NY, Pergamon.
14. I. E. REIMANIS, B. J. DALGLEISH, and A. G. EVANS: *Acta Metall. Mater.*, 1991, **39**, (12), 3133–3141.
15. C. F. SHIH and L. CHENG: Proc. Joint FEFG/ICF Int. Conf. on 'Fracture of engineering materials and structures', Singapore, August 1991, 41–49.
16. A. G. VARIAS, Z. SUO, and C. F. SHIH: *J. Mech. Phys. Solids*, 1991, **39**, (7), 963–986.
17. N. P. O'DOWD, C. F. SHIH, and M. G. STOUT: *Int. J. Solids Struct.*, 1992, **29**, (5), 571–589.
18. A. G. EVANS and B. J. DALGLEISH: *Acta Metall. Mater.*, 1992, **40**, S295–S306.
19. K.-H. SCHWALBE and M. KOÇAK: 'Mismatching of welds', European Structural Integrity Society Vol. 17; 1994, London, Mechanical Engineering Publications.
20. K.-H. SCHWALBE and M. KOÇAK: 'Mis-matching of interfaces and welds'; 1997, Geesthacht, Germany, GKSS Research Centre (ISBN 3–00–001951–00).
21. Y.-J. KIM, G. LIN, A. CORNEC, and K.-H. SCHWALBE: IIW Doc. X–F–022–95, presented at 2nd intermediate meeting of IIW subcommission X–F on 'Weld mis-match effect', GKSS Research Centre, Geesthacht, Germany, 1995.
22. Y.-J. KIM, G. LIN, A. CORNEC, and K.-H. SCHWALBE: IIW Doc. X–F–019–95, presented at 2nd intermediate meeting of IIW subcommission X–F on 'Weld mis-match effect', GKSS Research Centre, Geesthacht, Germany, 1995.
23. G. ÇAM, L. BUNGE, K.-H. BOHM, and M. KOÇAK: IIW Doc. X–F–076–98, Proc. 5th Int. Conf. on 'Trends in welding research', (ed. J. M. Vitek *et al.*), 669–676; 1999, Materials Park, OH, ASM International.
24. G. ÇAM, L. BUNGE, K.-H. BOHM, and M. KOÇAK: in 'Brazing, high temperature brazing and diffusion welding', DVS Bericht 192, 297–300; 1998, Düsseldorf, Germany, Deutscher Verlag für Schweißtechnik (DVS).
25. T. W. EAGER: *Weld. J.*, 1995, **74**, (6), 49–55.
26. G. ÇAM, M. KOÇAK, D. DOBI, L. HEIKINHEIMO, and M. SIREN: *Sci. Technol. Weld. Joining*, 1997, **2**, (3), 95–101.